An Autoregressive Model for Analysis of Ice Sheet Elevation Change Time Series

Adam C. Ferguson, *Member, IEEE*, Curt H. Davis, *Senior Member, IEEE*, and Joseph E. Cavanaugh

***Abstract*—In this paper, we present an autoregressive model that can effectively characterize both seasonal and interannual variations in ice sheet elevation change time series constructed from satellite radar or laser altimeter data. The AR model can be used in conjunction with weighted least squares regression to accurately estimate any longer term linear trend present in the cyclically varying elevation change time series. This approach is robust in that it can account for seasonal and interannual elevation change variations, missing points in the time series, signal aperiodicity, time series heteroscedasticity, and time series with a noninteger number of yearly cycles. In addition, we derive a theoretically valid estimate of the uncertainty (standard error) in the long-term linear trend. Monte Carlo simulations were conducted that closely emulated actual characteristics of five-year elevation change time series from Antarctica. The Monte Carlo results indicate that the autoregressive approach yields long-term linear trends that are less biased than two other approaches that have been recently used for analysis of ice sheet elevation change time series. In addition, the simulation results demonstrate that the variability (uncertainty) of the long-term linear trend estimates from the AR approach is in very good agreement with the derived theoretical standard error estimates.**

***Index Terms*—Autoregressive (AR) modeling, polar ice sheets, satellite altimetry, time series analysis.**

I. Introduction

TIME SERIES data of ice sheet surface elevation change can be constructed from satellite radar or laser altimeter data and used to study the mass balance of the polar ice sheets. Short-term changes in surface elevation occur both seasonally and interannually [1], while longer term elevation changes are linked to climate change and global sea level [2]. The European Space Agency's (ESA) European Remote Sensing 1 and 2 (ERS-1/2) satellite radar altimeters have provided nearly continuous measurement of surface elevation for the Greenland and Antarctic ice sheets up to latitudes $\pm 81.5^{\circ}$ since 1992. Wingham *et al.* [3] analyzed five-year elevation change time series of ERS-1/2 satellite radar altimetry data from 1992–1996 to show that the mass balance of the Antarctic ice sheet was not significantly different than zero. However, the ERS-1/2 elevation change results also showed that Pine Island Glacier (PIG) drainage was experiencing significant thinning, and results from an interferometric analysis of SAR imagery independently documented a recent 5-km retreat in the PIG grounding line with an 18% increase in the glacier speed [4]. The National Aeronautics and Space Administration (NASA) ICESat laser altimeter has commenced operation and is providing extended coverage of the polar ice sheets up to latitudes of $\pm 86^{\circ}$. In addition, ICESat will provide important new observations of ice sheet coastal areas and outlet glaciers where the satellite radar altimeter measurements are sparse and of limited utility.

Analysis of ice sheet elevation change time series from satellite altimetry is required for understanding important characteristics of the observed elevation change signal. This analysis is complicated by the fact that a typical elevation change time series will have a seasonal cycle superimposed upon a longer term trend. This cycle is due to seasonal variations in precipitation, snow densification, and surface melting (in some areas). In addition, it was recently demonstrated that seasonal variations in ice sheet flow can occur [5], and this can also contribute to seasonal elevation change signals in some areas. Moreover, interannual variations in these geophysical parameters further complicate the analysis and extraction of longer term trends related to mass balance change [1]. Appropriate characterization of seasonal and interannual elevation change variations is essential for reliable statistical evaluation of longer term trends.

In their analysis of five-year elevation change time series over Antarctica, Wingham *et al.* [3] used simple least squares linear regression, inversely weighted by the error variance of each sample, to estimate the long-term trend. However, this approach does not take into account the effect of seasonal or interannual variations in the elevation change signal. Zwally and Brenner [6] recently described an approach where a multivariate regression was used to fit a linear trend and a sine-cosine function with phase and amplitude as fixed parameters. In this approach, the amplitude of the seasonal cycle is held constant for the entire multiyear time series. Such a model, therefore, cannot account for interannual variations in the elevation signal. Since both of these approaches do not take into account important cyclical variations in the elevation change signal, error estimates obtained for the long-term linear trend from these methods may not be appropriate.

Here, we present an autoregressive (AR) model that can characterize seasonal and interannual variations in elevation change time series superimposed upon a long-term linear trend. In addition, we derive a theoretically valid estimate of the uncertainty in the long-term trend by using the AR model in conjunction with a weighted linear regression. Experimental results from Monte

Manuscript received June 9, 2003; revised August 14, 2004. This work was supported by the National Science Foundation under Grant NSF-OPP 9818734.

A. C. Ferguson is with the Radar Engineering Department, National Nuclear Security Administration, Kansas City, MO 64111 USA.

C. H. Davis is with the Department of Electrical and Computer Engineering, University of Missouri-Columbia, Columbia, MO 65211 USA (e-mail: DavisCH@missouri.edu).

J. E. Cavanaugh is with the Department of Biostatistics, University of Iowa, Iowa City, IA 52242 USA (e-mail: joe-cavanaugh@uiowa.edu).

Digital Object Identifier 10.1109/TGRS.2004.836788

Carlo simulations indicate that the autoregressive approach is less biased than the other approaches described above. In addition, the simulations validate the theoretical estimates of the uncertainty in the long-term linear trend. Thus, the autoregressive approach presented here is a robust and useful tool for modeling and analysis of ice sheet elevation change time series.

II. Elevation Change Time Series

Here, we briefly summarize an improved method used to generate ice sheet elevation change time series. This method was first presented in [7] and is summarized here for the sake of completeness as the nature of the ice sheet time series impacts the autoregressive modeling approach presented in the next section. In addition, several errors to equations given in [7] are corrected.

Individual elevation change estimates (dH) are computed from surface heights (H) at the intersection or crossover between time-separated ascending (H_A) and descending (H_D) satellite paths. The ascending–descending (AD) and descending–ascending (DA) elevation change estimates are formed separately as

$$dH_{\mathrm{AD}} = H_A(t_2) - H_D(t_1) + B_A - B_D \tag{1a}$$

$$dH_{\mathrm{DA}} = H_D(t_2) - H_A(t_1) + B_D - B_A \tag{1b}$$

where $dt = t_2 - t_1$ is always positive. The B_A and B_D terms represent possible time-invariant biases in the altimeter that result from directional dependencies in the orbit error and/or the scattering characteristics of the ice sheet [7], [8].

Satellite altimeter data are typically divided into monthly intervals and each month is compared or "crossed" with all other months to derive a complete crossover dataset from which a time series can be constructed. For N months of satellite data, the complete crossover dataset can be represented using a one-sided $N \times N dH$ matrix where each row represents the crossover data computed with respect to a different initial reference month

$$\overline{dH}_{i\times j} = \begin{bmatrix} \overline{dH}_{1\times 1} & \overline{dH}_{1\times 2} & \cdots & \cdots & \overline{dH}_{1\times N} \\ - & \overline{dH}_{2\times 2} & \overline{dH}_{2\times 3} & \cdots & \cdots \\ - & - & \cdots & \cdots & \cdots \\ - & - & - & \cdots & \cdots \\ - & - & - & - & \overline{dH}_{N\times N} \end{bmatrix}. \tag{2}$$

Each $\overline{dH}_{i\times j}$ matrix element represents the average elevation change between months i and j computed from an unbiased weighted average

$$\overline{dH}_{i\times j} = \frac{1}{n_T}[n_{\mathrm{AD}} \cdot \overline{dH}_{\mathrm{AD}} + n_{\mathrm{DA}} \cdot \overline{dH}_{\mathrm{DA}}]. \tag{3}$$

The corresponding standard error (SE) for each matrix element is given by

$$\mathrm{SE}_{i\times j} = \frac{1}{n_T}\sqrt{n_{\mathrm{AD}} \cdot \mathrm{SD}_{\mathrm{AD}}^2 + n_{\mathrm{DA}} \cdot \mathrm{SD}_{\mathrm{DA}}^2} \tag{4}$$

where $n_{\mathrm{AD}}, n_{\mathrm{DA}}$ are the number of AD and DA crossovers, $\mathrm{SD}_{\mathrm{AD}}$ and $\mathrm{SD}_{\mathrm{DA}}$ are the sample standard deviations for the dH_{AD} and dH_{DA} elevation differences, and $n_T = n_{\mathrm{AD}} + n_{\mathrm{DA}}$. An iterative three standard deviation editing procedure is used for the AD and DA crossovers separately for each matrix element to eliminate data outliers caused by irregular ice sheet topography.

Next, the $\overline{dH}_{i\times j}$ values in row 1 (reference row) for $j = 2$ to N are added to all elements of the corresponding matrix elements in row $i = j$ for all $j > i$, i.e.,

$$\overline{dH}'_{i\times j} = \overline{dH}_{1\times i} + \overline{dH}_{i\times j}, \qquad \text{for } i > 1; j = i+1 \text{ to } N. \tag{5}$$

This is done to insure that all matrix elements in (2) are referenced to the same initial time period (e.g., month 1). The resulting standard error for each element is then

$$\mathrm{SE}'_{i\times j} = \sqrt{\mathrm{SE}_{1\times j}^2 + \mathrm{SE}_{i\times j}^2}, \qquad \text{for } i > 1; j = i+1 \text{ to } N. \tag{6}$$

For the reference row, the SE remains the same as that given in (4), but to maintain consistent notation, $\mathrm{SE}'_{i\times j}$ will be used to represent the revised SE for all matrix elements. Once every matrix element is referenced to the same initial time period, each column in the dH matrix (2) can be averaged to form a single value for each month. As in (3), an unbiased weighted average is constructed where the weights are proportional to the number of samples in each matrix element. When the dH matrix is referenced to the appropriate time period, a revised number of crossover points in each element must be computed

$$n'_{i\times j} = n_{1\times j} + n_{i\times j}, \qquad \text{for } i > 1; j = i+1 \text{ to } N. \tag{7}$$

The total number of crossovers in each column of the dH matrix is then

$$n_j = \sum_{i=1}^{j} n'_{i\times j}, \qquad \text{for } j = 1 \text{ to } N. \tag{8}$$

A weighted average is then computed for each column in the dH matrix

$$\overline{dH}_j = \sum_{i=1}^{j} (w_{i\times j} \cdot \overline{dH}'_{i\times j}), \qquad \text{for } j = 1 \text{ to } N \tag{9}$$

where the weight for each matrix element is given by $w_{i\times j} = n'_{i\times j}/n_j$. The corresponding SE for each column average is then

$$\mathrm{SE}_j = \sqrt{\sum_{i=1}^{j} (w_{i\times j} \cdot \mathrm{SE}'_{i\times j})^2}, \qquad \text{for } j = 1 \text{ to } N. \tag{10}$$

We note that (3), (9), and (10) include corrections to corresponding equations given in [7] that contain errors.

The final result given in (9) is an improved N-point dH time series that is formed using all available crossover data. The conventional method used for forming elevation change time series from altimeter data only utilizes a single reference time period (e.g., [3]). This is equivalent to using only a single row of crossover data in the dH matrix given in (2), and consequently only a fraction of the available crossover data are utilized. By referencing each row in the dH matrix (5) to a common time period, a weighted column average can be formed using all crossover data. This approach: 1) dramatically increases the

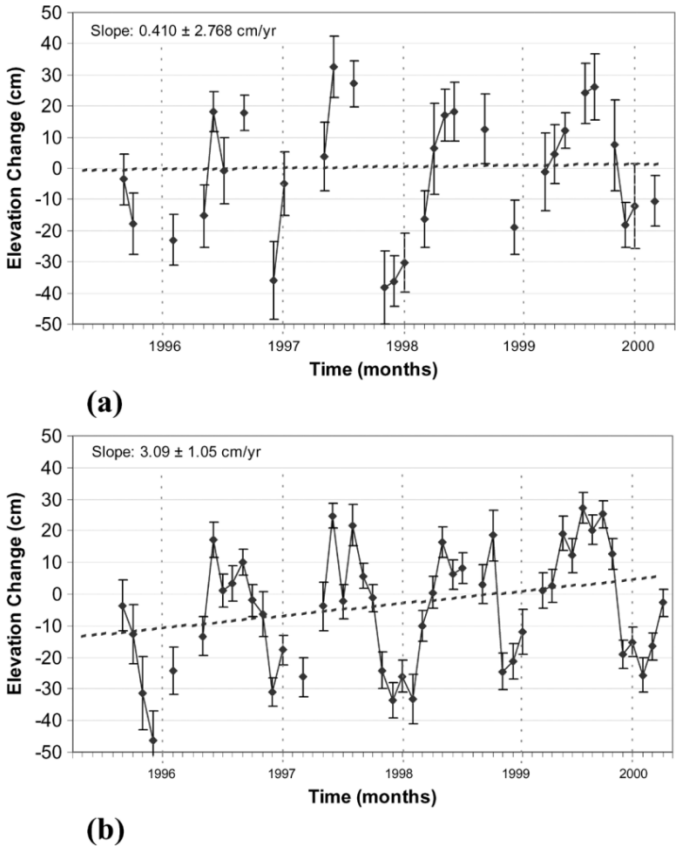

Fig. 1. Comparison between (a) conventional and (b) improved time series method for a five-year elevation change time series from [9] constructed for $1^\circ \times 2^\circ$ region in east Antarctica centered at 70.5° S, 45° E. The conventional and improved time series methods utilize 443 and 18 987 dH measurements, respectively.

number of elevation change estimates used in forming the time series; 2) reduces the amount of gaps (no data) in the time series; and 3) significantly reduces the error estimates for most of the individual dH estimates.

Fig. 1 presents a comparison between the conventional and improved method for a five-year elevation change time series constructed for a $1^\circ \times 2^\circ$ region in east Antarctica [9]. Note that a strong seasonal cycle is superimposed about a longer term linear trend. Fig. 1(a) shows the conventional method where only 443 crossover data points are used in the formation of the time series. As one can see, there are a large number of gaps and most error bars are relatively large. Fig. 1(b) shows the time series formed from the improved method where 18 987 total crossover data points are used. This is about 43 times the number of points used in the conventional method. Consequently, the improved time series has 18 additional monthly dH measurements and significantly smaller standard errors on most dH points common to both time series. Also, a significantly different long-term elevation trend is obtained (estimated using the autoregressive technique described in the next section), and the standard error for the long-term trend is 1.7 cm/year smaller than that obtained from the conventional method.

Finally, it is important to note several issues related to instrumental dependencies of ice sheet surface elevation measurements from satellite radar altimeters. Time-invariant AD biases [B_A and B_D in (1)] occur in linearly polarized radar altimeter data (e.g., ERS-1/2) due to variations in backscattered power caused by directional anisotropy [8], [10]. Such biases are not present in circularly polarized radar altimeter data (e.g., Seasat, Geosat) [8], [11]. Directional anisotropy effects are stable over time [10] and can, therefore, be canceled out by averaging dH_{AD} and dH_{DA} elevation differences (1) together as is done in (3) [7], [10]. Also, seasonal variations in surface backscattered power can cause spurious time-varying changes in linearly polarized radar altimeter measurements of ice sheet surface elevation [3], [9], [10], [12]. A discussion of the seasonal backscatter variation and correction for its influence on longer term elevation change estimates is provided in [9] for five-year ERS-2 time series from Antarctica. Backscatter-dependent seasonal variations in surface elevation have not, thus far, been documented in circularly polarized radar altimeter data [11].

III. AR Time Series Model

A. Traditional Regression Methods

Two fitting methods commonly used in linear regression are the weighted least squares (WLS) and the chi-squared procedures. Both methods are normally implemented by standardizing the original data and then fitting a linear trend using ordinary least squares (OLS). In the present setting, these two methods are appealing because they can account for the heteroscedastic nature of the data, i.e., the fact that each point in the time series has a different standard error (e.g., Fig. 1). Basically, points with a small standard error are given more weight than points with a large standard error. However, an underlying assumption in these methods is that the data can be described by Gaussian white noise about a linear trend. Thus, residuals from the standardized model fit should be approximately independent, identically distributed Gaussian variates with a zero mean and constant variance, i.e., approximately independent identically distributed (i.i.d.) $N(0, \sigma^2)$.

The residuals associated with the standardized model are effectively differences between the standardized data values and the estimated linear trend. A strong correlation between adjacent residuals will exist for ice sheet elevation change time series due to the seasonal cycle that is superimposed upon the longer term trend (if present). Therein lies the major flaw that makes weighted least squares and chi-squared algorithms inappropriate for ice sheet elevation change time series. Unaccounted for seasonal and interannual signals can significantly alter linear trend estimates derived from the WLS and chi-squared approaches. Equally important, the i.i.d. $N(0, \sigma^2)$ assumption will cause the standard error assigned to the linear trend to be significantly larger than its actual value because the residual variance will contain components due to white noise and the seasonal/interannual cyclical variability. By neglecting key characteristics of the ice sheet time series, linear trends estimated from the data cannot be recovered as accurately as they would when using a model that accounts for the seasonal cycle, interannual variability, and the linear trend.

B. Autoregressive Methodology

A valid statistical model capable of accounting for periodic characteristics of serial data is an autoregressive (AR) model.

An AR model of order M describes cyclic behavior by expressing each point as an additive combination of M past points and an error component, $\varepsilon(t)$. For example, an AR model of order two, $\mathrm{AR}(2)$, would have the form

$$x(t) = \phi_1 \cdot x(t-1) + \phi_2 \cdot x(t-2) + \varepsilon(t) \tag{11a}$$

and an AR model of order M could be written as

$$x(t) = \phi_1 \cdot x(t-1) + \phi_2 \cdot x(t-2) + \phi_3 \cdot x(t-3) + \cdots \phi_M \cdot x(t-M) + \varepsilon(t). \tag{11b}$$

Intuitively, the problem of characterizing a seasonal cycle oscillating about a linear trend can be handled by a combination of an autoregressive model to describe the cycle, and a linear regression model to describe the linear trend (fit using WLS when heteroscedasticity exists in the data). By utilizing an autoregressive model as part of a larger framework, systematic short- and medium-term variations in the data can be accounted for and the linear trend can be more accurately estimated from the ice sheet elevation change time series.

Cochrane and Orcutt [13] first proposed an iterative technique based on the method of maximum likelihood for fitting data consisting of both a cycle and linear trend. Shumway and Stoffer [14] provide an updated summary of the algorithm. This approach must be modified in the current setting to properly account for known characteristics of ice sheet elevation change time series. These modifications were designed using accepted statistical techniques and methodologies. First, the heteroscedastic nature of the data must be addressed. This is done by standardizing the data. Second, most ice sheet elevation change time series will have missing data points due to poor coverage, instrument limitations, and/or quality filtering done in the data processing chain. The method for filling gaps in the time series is discussed in Section III-D. Here, we first present the complete algorithm assuming no gaps exist in the time series.

Our base model is assumed to be

$$y_i = \alpha + \beta \cdot x_i + e_i \tag{12a}$$

where x_i represents the time index corresponding to point i, $\alpha + \beta \cdot x_i$ describes the long-term trend, and e_i characterizes the seasonal and interannual signal variations. Assuming an $\mathrm{AR}(2)$ may be used to model e_i, we would have

$$e_i = \phi_1 \cdot e_{i-1} + \phi_2 \cdot e_{i-2} + k_i \cdot w_i \tag{12b}$$

where $w_i \sim \text{i.i.d.} N(0, \sigma^2)$, and k_i is a heteroscedasticity factor that regulates the variability at point i.

The methodology can be broken into five distinct steps:

Step 1) An initial line is fit to the time series using a common multiple linear regression technique: OLS on the standardized data (this is equivalent to WLS). Here, the heteroscedasticity of the data is handled by first standardizing each data point with respect to its own standard error. Equation (13) presents the general form and notation for the standardized data where $i = 1, \ldots, N$, and N is the total number of samples in the time series

$$x_i^* = \frac{x_i}{\mathrm{SE}_i} \quad y_i^* = \frac{y_i}{\mathrm{SE}_i} \quad z_i^* = \frac{1}{\mathrm{SE}_i}. \tag{13}$$

The standardized model is then represented by

$$y_i^* = \alpha \cdot z_i^* + \beta \cdot x_i^* + \varepsilon_i^* \tag{14}$$

and initial estimates of α and β are obtained using OLS.

Step 2) Next, the seasonal cycle is modeled by first subtracting the initial linear trend fit in Step 1) from the standardized data. This essentially leaves the seasonal cycle and a small residual linear trend that could not be accurately captured in Step 1). Now, an AR model is fit to the seasonal cycle. The AR parameters $\hat{\phi}_1, \hat{\phi}_2, \ldots, \hat{\phi}_M$ can be found by conditional or unconditional maximum likelihood estimation, conditional or unconditional least squares, or an alternative method. We used conditional least squares, which is equivalent to conditional maximum likelihood under normality of the model residuals [15, pp. 53–55].

Step 3) A transformed time series is then derived using the AR parameters. The transformation basically removes the cyclic trend modeled in Step 2) from the original standardized data. Thus, a linear trend and white noise are left. For example, the transformed data based on an $\mathrm{AR}(2)$ model would be found using the equations

$$\begin{aligned} x_i^{**} &= x_i^* - \hat{\phi}_1 \cdot x_{i-1}^* - \hat{\phi}_2 \cdot x_{i-2}^* \\ y_i^{**} &= y_i^* - \hat{\phi}_1 \cdot y_{i-1}^* - \hat{\phi}_2 \cdot y_{i-2}^* \\ z_i^{**} &= z_i^* - \hat{\phi}_1 \cdot z_{i-1}^* - \hat{\phi}_2 \cdot z_{i-2}^*. \end{aligned} \tag{15}$$

Step 4) Now, using the transformed series, a new linear model

$$y_i^{**} = \alpha \cdot z_i^{**} + \beta \cdot x_i^{**} + w_i \tag{16}$$

is fit using OLS [as in Step 1)]. It is important to note that the time series data are not standardized this time because they remain standardized from Step 1). By performing this step, more accurate estimates for the intercept $(\hat{\alpha})$, slope $(\hat{\beta})$, and their corresponding standard errors $(\mathrm{SE}_{\hat{\alpha}}, \mathrm{SE}_{\hat{\beta}})$ can be obtained.

Step 5) Finally, the preceding four steps are performed for AR models of various orders. The best model is chosen by finding the fitted model that minimizes the Akaike Information Criterion (AIC) [16]. The AIC is a scoring function commonly used for statistical model selection. The criterion is formed by adding a cost for each increase in the model order and deducting a cost for an improved fit of the

model to the data. In our application, we define the AIC as

$$\mathrm{AIC} = m \cdot \ln\left(\frac{m-2}{m} \cdot \hat{\sigma}^2_{y**}\right) + 2 \cdot (M+2). \tag{17}$$

Here, the first term is the goodness-of-fit term, the second term is the penalty term, $\hat{\sigma}^2_{y**}$ is the residual mean square associated with the fitted model, M is the order of the AR model under consideration, and $m = N - M^*$, where N is total number of time series points in the original data, and M^* is the highest order AR model to be compared.

Intuitively, one might be tempted to choose the model that best conforms to the available data. However, the goal in statistical modeling is to accurately describe the phenomenon that yields the data, not to merely describe the data at hand. By adding more and more parameters to a model, one can always improve the conformity of the fitted model to the available data. However, an unnecessarily complex model may provide an inappropriate description of the associated phenomenon, and hence do a poor job of characterizing a different set of data produced by the same phenomenon. Effectively, the AIC chooses the AR model that provides the optimal compromise between fidelity to the data and parsimony.

C. Standard Error of the Linear Trend

The standardized AR model given in (14) can be written in matrix form as

$$\begin{bmatrix} y_1^* \\ \cdot \\ \cdot \\ \cdot \\ y_N^* \end{bmatrix} = \begin{bmatrix} z_1^* & x_1^* \\ \cdot & \cdot \\ \cdot & \cdot \\ \cdot & \cdot \\ z_N^* & x_N^* \end{bmatrix} \times \begin{bmatrix} \alpha \\ \beta \end{bmatrix} + \begin{bmatrix} \varepsilon_1^* \\ \cdot \\ \cdot \\ \cdot \\ \varepsilon_N^* \end{bmatrix} \tag{18a}$$

or

$$\mathrm{Y}^* = \mathrm{X}^* \times \mathrm{B} + \mathrm{E}^*. \tag{18b}$$

Assume that $\mathrm{Var}(\mathrm{E}^*) = \sigma^2 \times I$, where I is the identity matrix. This implies that ε_i are uncorrelated. Under this assumption, the model can be fit using OLS. The OLS estimator of the vector B is given by

$$\hat{\mathrm{B}} = (\mathrm{X}^{*'} \times \mathrm{X}^*)^{-1} \times \mathrm{X}^{*'} \times Y^* \tag{19}$$

and the variance/covariance matrix of $\hat{\mathrm{B}}$ by

$$\mathrm{Var}(\hat{\mathrm{B}}) = \mathrm{Var}((\mathrm{X}^{*'} \times \mathrm{X}^*)^{-1} \times \mathrm{X}^{*'} \times \mathrm{Y}^*). \tag{20}$$

Note that the preceding can be written as

$$\mathrm{Var}(\hat{\mathrm{B}}) = [(\mathrm{X}^{*'} \times \mathrm{X}^*)^{-1} \times \mathrm{X}^{*'}] \times \mathrm{Var}(\mathrm{Y}^*) \cdot [\mathrm{X}^* \cdot (\mathrm{X}^{*'} \cdot \mathrm{X}^*)^{-1}]. \tag{21}$$

Suppose the assumption that $\mathrm{Var}(\mathrm{E}^*) = \sigma^2 \cdot I$ is correct. Then, $\mathrm{Var}(\mathrm{Y}^*) = \sigma^2 \cdot I$, and (21) reduces to

$$\mathrm{Var}(\hat{\mathrm{B}}) = \sigma^2 \cdot (\mathrm{X}^{*'} \cdot \mathrm{X}^*)^{-1}. \tag{22}$$

On the other hand, suppose the assumption $\mathrm{Var}(\mathrm{E}^*) = \sigma^2 \cdot I$ is incorrect. Specifically, suppose that $\mathrm{Var}(\mathrm{E}^*) = \sigma^2 \cdot V$, where V is positive definite. A positive definite matrix is symmetric and invertible, with an inverse that can be written in the form $V^{-1} = V^{-1/2} \cdot V^{-1/2}$. Here, $V^{-1/2}$ is symmetric, invertible, and satisfies $V^{-1/2} \cdot V \cdot V^{-1/2} = I$. Then, $\mathrm{Var}(Y^*) = \sigma^2 \cdot V$, and (21) reduces to

$$\mathrm{Var}(\hat{\mathrm{B}}) = [(\mathrm{X}^{*'} \times \mathrm{X}^*)^{-1} \times \mathrm{X}^{*'}] \times [\sigma^2 \times V] \cdot [\mathrm{X}^* \times (\mathrm{X}^{*'} \times \mathrm{X}^*)^{-1}] \tag{23a}$$

$$\mathrm{Var}(\hat{\mathrm{B}}) = \sigma^2 \times (\mathrm{X}^{*'} \times \mathrm{X}^*)^{-1} \times [\mathrm{X}^{*'} \times V \times \mathrm{X}^*] \cdot (\mathrm{X}^{*'} \times \mathrm{X}^*)^{-1}. \tag{23b}$$

Adoption of the V matrix implicitly acknowledges the fact that ε_i are correlated.

Inherently, the autoregressive model assumes that ε_i are correlated, which is appropriate in the application at hand due to the seasonal cycle in the ice sheet elevation change time series. Thus, $\mathrm{Var}(\mathrm{E}^*) = \sigma^2 \times V$. Writing $V^{-1} = V^{-1/2} \times V^{-1/2}$, we can obtain a matrix representation of the model given in (16) by considering the following transformations:

$$V^{-\frac{1}{2}} \times \begin{bmatrix} z_1^* & x_1^* \\ \cdot & \cdot \\ \cdot & \cdot \\ \cdot & \cdot \\ z_N^* & x_N^* \end{bmatrix} = \begin{bmatrix} z_1^{**} & x_1^{**} \\ \cdot & \cdot \\ \cdot & \cdot \\ \cdot & \cdot \\ z_N^{**} & x_N^{**} \end{bmatrix} \tag{24a}$$

or

$$V^{-\frac{1}{2}} \times \mathrm{X}^* = \mathrm{X}^{**} \tag{24b}$$

and

$$V^{-\frac{1}{2}} \times \begin{bmatrix} y_1^* \\ \cdot \\ \cdot \\ \cdot \\ y_N^* \end{bmatrix} = \begin{bmatrix} y_1^{**} \\ \cdot \\ \cdot \\ \cdot \\ y_N^{**} \end{bmatrix} \tag{25a}$$

or

$$V^{-\frac{1}{2}} \times Y^* = Y^{**}. \tag{25b}$$

Now, the model given in (18) can be transformed as

$$\left(V^{-\frac{1}{2}} \times \mathrm{Y}^*\right) = \left(V^{-\frac{1}{2}} \times \mathrm{X}^*\right) \times \mathrm{B} + \left(V^{-\frac{1}{2}} \times \mathrm{E}^*\right) \tag{26}$$

to yield

$$\mathrm{Y}^{**} = \mathrm{X}^{**} \times \mathrm{B} + \mathrm{E}^{**}. \tag{27}$$

Notice that (27) is exactly the same as (16) presented in Step 4) of Section III-B. We now have

$$\begin{aligned} \mathrm{Var}(\mathrm{E}^{**}) &= \mathrm{Var}\left(V^{-\frac{1}{2}} \times \mathrm{E}^*\right) \\ &= V^{-\frac{1}{2}} \times \mathrm{Var}(\mathrm{E}^*) \times V^{-\frac{1}{2}'} \\ &= V^{-\frac{1}{2}} \times (\sigma^2 \times V) \times V^{-\frac{1}{2}'} \\ &= \sigma^2 \times \left(V^{-\frac{1}{2}} \times V \times V^{-\frac{1}{2}}\right) \end{aligned} \tag{28a}$$

and therefore

$$\mathrm{Var}(\mathrm{E}^{**}) = \sigma^2 \times \mathrm{I}. \tag{28b}$$

Thus, E^{**} is white, meaning the model presented in Step 4) of Section III-B can be appropriately fit using OLS. The OLS estimator of B is given by

$$\hat{\mathrm{B}} = (\mathrm{X}^{**'} \times \mathrm{X}^{**})^{-1} \times \mathrm{X}^{**'} \times \mathrm{Y}^{**} \tag{29}$$

and the variance/covariance matrix for $\hat{\mathrm{B}}$ by

$$\mathrm{Var}(\hat{\mathrm{B}}) = \mathrm{Var}((\mathrm{X}^{**'} \times \mathrm{X}^{**})^{-1} \times \mathrm{X}^{**'} \times \mathrm{Y}^{**}) \tag{30a}$$

$$\mathrm{Var}(\hat{\mathrm{B}}) = \sigma^2 \times (\mathrm{X}^{**'} \times \mathrm{X}^{**})^{-1}. \tag{30b}$$

The standard error for the autoregressive linear trend, $\mathrm{SE}_{\hat{\beta}}$, can be obtained directly from (30b). Its value will always be less than that obtained from (23). This fact can be established as a consequence of the Gauss–Markov Theorem (see [17, Th. 2.7.1, pp. 29–30]). Thus, the AR approach for modeling the seasonal/interannual cyclical variations in the elevation change time series will lead to more accurate estimates of longer term linear trends, if present, in the time series.

The AR model accurately characterizes the salient features of the vast majority of ice sheet elevation change time series we have observed. However, some longer term time series trends exhibit obvious nonlinear variations, rendering the linear component of the AR model invalid. In instances where a nonlinear trend deviates substantially from the linear description provided by the AR model, the deviation will be reflected in the difference between the model fit (16) and the time series data. Thus, the residual variance will reflect not only white noise variability but also the structural impropriety of the linear model adopted for the longer term trend. The estimated standard error for the autoregressive linear trend obtained via (30b) will, therefore, be large due to the inflated estimate of σ^2. This will provide protection from making erroneous inferential conclusions pertaining to the average rate of change estimated over the time series duration.

D. Time Series Gap Filling

When a gap exists in the elevation change time series (e.g., Fig. 1), the algorithm presented in Section III-C will have problems. Since Step 3) transforms the current data using the estimated AR coefficients and previous data, an erroneous result will occur if some of the previous data are missing. For example, if one were using an $\mathrm{AR}(2)$ model to transform a series and sample number 9 (y_9^*) in the series was missing, the transformed data corresponding to points 9, 10, and 11 $(y_9^{**}, y_{10}^{**}, y_{11}^{**})$ would be errant, since

$$\begin{aligned} y_9^{**} &= y_9^* - \hat{\phi}_1 \cdot y_8^* - \hat{\phi}_2 \cdot y_7^* \\ y_{10}^{**} &= y_{10}^* - \hat{\phi}_1 \cdot y_9^* - \hat{\phi}_2 \cdot y_8^* \\ y_{11}^{**} &= y_{11}^* - \hat{\phi}_1 \cdot y_{10}^* - \hat{\phi}_2 \cdot y_9^*. \end{aligned} \tag{31}$$

To overcome this obstacle, an iterative procedure is used to estimate missing elevation change data wherever possible. First, after Step 1), the missing data positions are filled with estimates that lie on the initial linear regression model fit. The AR coefficients are then found, as required in Step 2). These initial AR parameters are subsequently used to estimate data values in the missing locations. The estimates of the missing values are then used to complete the data, Steps 1) and 2) are reexecuted, and updated estimates are constructed for the data values in the missing locations. An iterative approach is employed because the gaps are first filled using points on the initial linear fit, and these are likely to deviate substantially from the seasonal cycle. By iterating through several estimates for the gaps, elevation change estimates that are consistent with the seasonal cycle will eventually be used to fill the gaps.

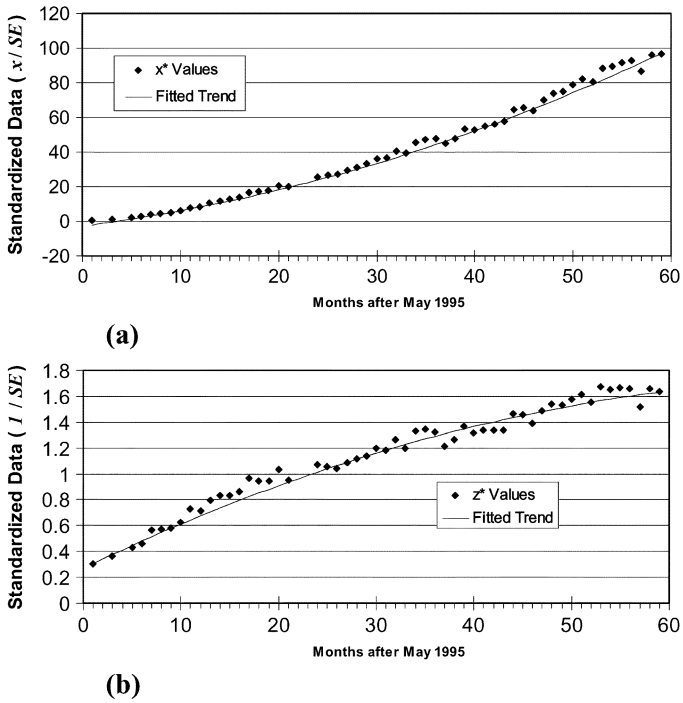

Fig. 2. Standardized (a) x_i^* and (b) z_i^* data series from a $0.6^\circ \times 2^\circ$ region centered at 81.3° S, 1° E in east Antarctica (see Fig. 3). A simple second-order polynomial model can accurately describe the standardized data series.

To illustrate, assume we are using an $\mathrm{AR}(2)$ model to transform a time series and sample number 9 (y_9^*) in the series is missing. An initial estimate for the AR parameters would be found based on the actual data with the addition of an estimated value for sample 9 (y_9^*) that is obtained by selecting the point on the first-pass fitted linear regression model. Then, these AR parameters are used to estimate a new value for y_9^*, i.e.,

$$y_9^* = \hat{\phi}_1 \cdot y_8^* + \hat{\phi}_2 \cdot y_7^*. \tag{32}$$

This procedure is repeated until the value estimated for y_9^* varies by less than 2% between consecutive iterations. For multiple gaps, the percent change for each estimated gap is computed and the average percent change of all gaps must be less than 2% for convergence.

It is also necessary to estimate x_i^* and z_i^* where gaps exist. These values can be estimated by taking advantage of known trends in the x_i^* and z_i^* series. A key characteristic of the improved time series method presented in Section II is that the SE_i series follows a rather predictable trend. Namely, the SE_i values tend to decrease with increasing time because the weighted column average formed from the dH matrix (2) described in Section II will generally use more samples with increasing time. Noting this fact and recalling that $x_i^* = x_i/\mathrm{SE}_i$ and $z_i^* = 1/\mathrm{SE}_i$ (13), it is easy to see that a trend should exist in the x_i^* and z_i^* series as well. These assumptions are justified by actual data. Fig. 2 shows x_i^* and z_i^* series from a $0.6^\circ \times 2^\circ$

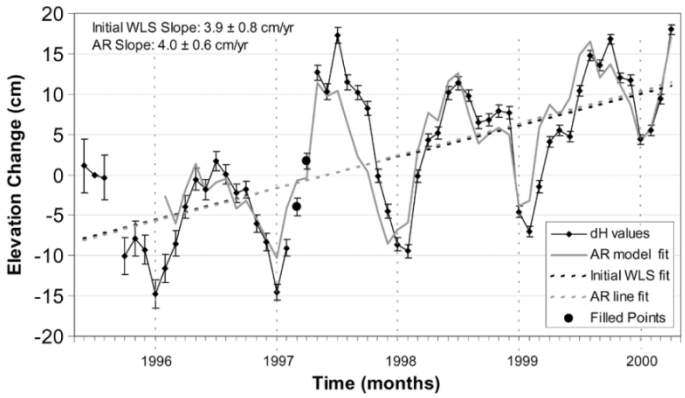

Fig. 3. Elevation change time series for a $0.6° \times 2°$ region centered at 81.3° S, 1° E in east Antarctica. The gap-filling procedure (Section III-D) has been used to fill in missing points corresponding to March and April of 1997 (indices 22 and 23 in Fig. 2). Note that the gap-filled elevation change estimates follow the observed seasonal cycle. The AIC chose a sixth-order AR model for the cyclical fit.

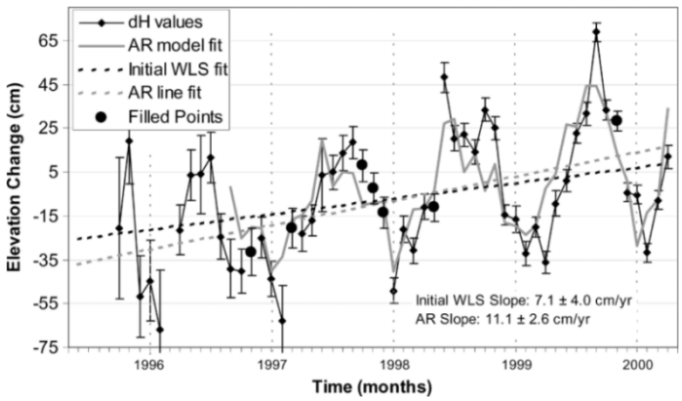

Fig. 4. Elevation change time series for a $1° \times 2°$ region centered at 71.5° S, 77° E in east Antarctica. Note that the gap-filled elevation change estimates follow the observed seasonal cycle. The AIC chose a fifth-order AR model for the cyclical fit. Note the difference between the WLS and AR slope estimates.

region centered at 81.3° S, 1° E in east Antarctica. As the figure demonstrates, a simple second-order polynomial model can accurately describe the series. This simple model can, therefore, be used to fill gaps in the x_i^* and z_i^* series so that the AR model parameters can then be used to obtain realistic elevation change estimates for the missing points. Fig. 3 shows the elevation change time series where this procedure has been used to fill in missing points at indices 21 and 22 (Fig. 2). Note that the gap-filled elevation change estimates closely follow the observed seasonal cycle.

There are gaps that cannot be filled using forward processing of the time series data due to their locations in the series and/or the level of the AR model being used. However, in general these tend to occur in the first several samples of typical ice sheet elevation change time series. For instance, if one were using an $\mathrm{AR}(5)$ model, it would be impossible to use the aforementioned procedure to find an estimate for a gap at y_4^*. This is because five samples prior to y_4^* are required for the iterative procedure to work. In such cases, the time series is truncated so that the beginning of the series is defined as the data point after the latest (highest index) gap, and an AR model is fit to the truncated time series. We note that *reverse* processing of the time series, where the sample order is inverted (e.g., $\mathrm{first\ sample} \rightarrow \mathrm{last\ sample}, \mathrm{second\ sample} \rightarrow \mathrm{next\ to\ last\ sample}$, etc.), can be used to fill points near the beginning of the time series that cannot be filled using forward processing as described above. We did not implement this here as the error bars near the beginning of the time series are generally 3–5 times larger than those at the end (e.g., see Fig. 3).

It is important to note that a limitation of the autoregressive algorithm is that, in rare instances, a model could be fit using only a small amount of the available data in the time series. This happens in situations where there are gaps late in the series that cannot be filled and the algorithm truncates the time series to be fit (as described above). Also, even if gaps that cannot be filled exist relatively early in the series, the AIC could pick a higher order model and the fitting would begin on the data point in the truncated series corresponding to the AR model order (e.g., if the time series is truncated to begin at index 12 and an $\mathrm{AR}(12)$ model is picked, the model fit starts at index 24). Thus, appropriate checks must be incorporated into the algorithm to ensure that a sufficient number of the time series points are actually used for the application at hand.

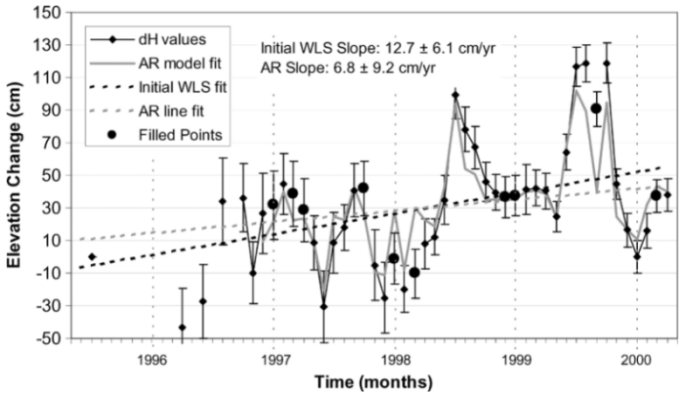

Fig. 5. Elevation change time series for a $1° \times 2°$ region centered at 68.5° S, 99° E in east Antarctica. The AIC chose a second-order AR model for the cyclical fit. Note that the WLS slope estimate is biased to a higher value than the AR model slope because of the strong aperiodic positive seasonal signal swings in the latter part (1998 and 1999) of the time series.

IV. Results and Discussion

A. Sample Autoregressive Model Fits

The autoregressive methodology described in the preceding section yields visually appealing and statistically accurate fits to actual ice sheet elevation change time series exhibiting a wide variety of conditions. Figs. 3–5 demonstrate that the AR algorithm does a good job of modeling elevation change time series regardless of missing data, indefinite seasonal cycle, or substantial seasonal and interannual signal variations. Note that the gap-filled dH points in these figures closely follow the observed seasonal signal in the vicinity of each point. This enables an appropriate AR model to be constructed for the elevation change time series. Without an appropriate gap-filling methodology, the success of the AR approach would be compromised in time series where a significant number of gaps are distributed uniformly throughout the time series (e.g., Fig. 5).

The slope and standard error estimates from the AR technique are compared to the initial WLS slope and SE estimates, and these values are listed on each figure. These two approaches are

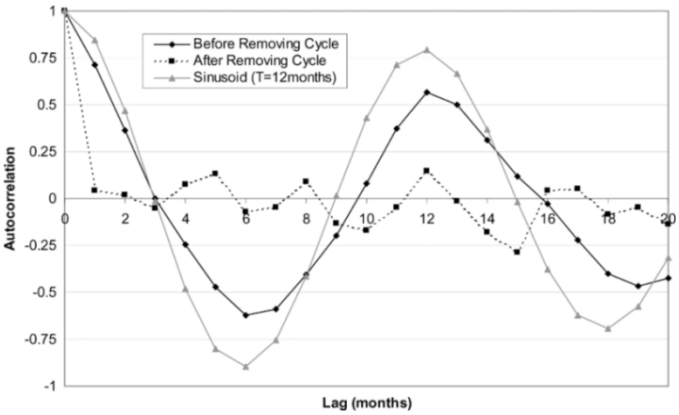

Fig. 6. Autocorrelation of residuals from the elevation change time series shown in Fig. 3 before and after fitting the AR model to estimate the seasonal cycle. Also shown is the autocorrelation of a sinusoid (12-month period) of length equal to that of the time series (five years).

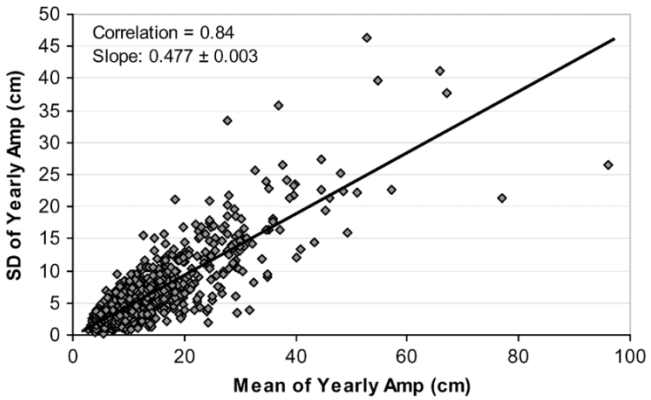

Fig. 7. Scatter plot showing the strong relationship between the mean yearly amplitude and the SD of the yearly amplitude for five-year elevation change time series from Antarctica [9].

compared while keeping in mind that the slope standard error estimates from the initial WLS model are computed assuming uncorrelated residuals, which in practice yields unreliable results. For this reason, the actual improvement in the standard error obtained using the AR model cannot be quantified. The development in Section III-C illustrates the inherent problem: if the initial WLS model (without the AR adjustment) is assumed to be correct, standard errors will be constructed using the incorrect variance/covariance matrix given by (22). However, the variance/covariance matrix in (23) is appropriate since the development of (23) acknowledges the seasonal cycles whereas the development of (22) does not.

Fig. 3 shows the elevation change time series for the same region as the x_i^* and z_i^* plots provided in Fig. 2. Note that the AR model effectively captures the substantial interannual variability in the seasonal cycle. However, in this region the difference between the WLS slope and the AR slope is small. Figs. 4 and 5 show examples of time series where the estimated slope varies significantly between the WLS model alone and the AR model. In particular, the WLS slope in Fig. 5 is biased to a higher value than the AR model slope because of the strong aperiodic positive seasonal signal swings in the latter part of the time series. These figures effectively demonstrate that utilizing the autoregressive model to remove the seasonal/interannual signals can yield a noticeably different linear fit. Whenever there are missing time series data, only quasiperiodic seasonal variations, or strong interannual variations in the seasonal cycle there is greater likelihood that a WLS linear trend will be erroneous.

The assumption of Gaussian white noise is inherent in the standard error estimates obtained from both the AR approach (Section III-C) and the WLS approach. However, this assumption is only valid for the AR approach because it effectively models the seasonal cycle and removes the cycle before the linear trend is estimated. Fig. 6 shows the autocorrelation of the elevation change time series from Fig. 3. The autocorrelation of the time series after removal of the cyclical signal via the AR model approximates that of a delta function, which is the theoretical autocorrelation function of a white noise process. Conversely, the autocorrelation of the time series before removal of the cyclical signal clearly approximates that of a sinusoidal time series with a period of twelve months. The final linear fit using the AR algorithm is performed using time series data that are much more "white" than the data used for the initial WLS fit, because the former corresponds to an autocorrelation graph that displays little, if any, periodicity. Thus, the transformation based on the AR model effectively acts as a prewhitening filter prior to the linear trend estimation. This is the statistical basis for adopting the autoregressive approach, enabling a theoretically viable estimate of the uncertainty associated with the linear trend to be obtained.

B. Monte Carlo Simulations

In order to validate the AR methodology, Monte Carlo simulations were conducted to further test the AR approach against other regression methods. For the base simulation, sample time series were generated with a length corresponding to five years (e.g., $N = 60$ monthly samples). The mean amplitude for each simulated yearly cycle was selected based on a random process defined by the amplitude distribution of actual five-year elevation change time series generated for $1^\circ \times 2^\circ$ regions from ERS-2 Antarctica data [9], [18]. The distribution of the observed regional mean amplitudes was approximately Rayleigh, and typical mean amplitude values ranged between 5–25 cm [18].

The standard deviation (SD) of the yearly amplitudes (interannual variability) was estimated by examining the relationship between the mean yearly amplitude and its standard deviation from the observed five-year time series. Fig. 7 shows a strong linear relationship between the mean yearly amplitude and the SD of the yearly amplitude. A least squares fit to the data (0.84 correlation) demonstrates that the SD of the yearly amplitude can be approximated as ~ 0.5 times the mean yearly amplitude. This relationship was used to select the SD of the yearly amplitude for the Monte Carlo simulations.

The selected mean and standard deviation for the time series amplitudes were used as the mean and standard deviation of a Gaussian distribution to generate the actual year-to-year amplitude values for each simulated time series. Mirroring actual five-year ERS-2 time series in [9], six amplitudes were picked for the base simulation from this Gaussian distribution corresponding to four full years and two half years. For all simulated series, these amplitudes were applied to a sine function with a 12-month period. The standard error function describing the error at each time series point decreased with increasing time

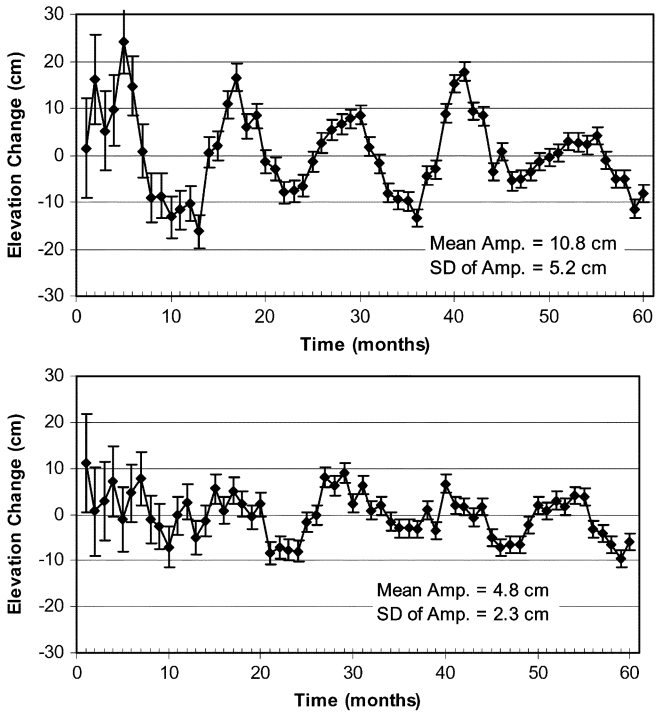

Fig. 8. Sample Monte Carlo generated zero-slope time series with sinusoidal cycle, white noise, and interannual amplitude variability (based on a standard deviation which is 0.5 times the average cycle amplitude; Fig. 7). The random error (white noise) decreases with time to mimic actual time series generated using the improved time series method described in Section II.

due to reasons discussed in previous sections. The adopted SE function was the same for all simulated series. The SE function versus time was defined using a model fit to actual standard error versus time data [18]. In general, the standard errors of actual time series decay exponentially to some minimum (nonzero) value [18]. Finally, white noise for each time series point was generated from a zero-mean Gaussian distribution with standard deviation equal to that point's standard error. Fig. 8 shows two simulated time series generated using these procedures.

For each mean yearly amplitude and standard deviation value, 500 Monte Carlo simulated time series were generated and fit using three different methods: weighted least squares (WLS), autoregressive (AR), and multivariate sinusoidal regression (MSR). The MSR iteratively fits a constant amplitude sinusoidal model plus linear trend described by Zwally and Brenner [6] where

$$dH(t) = A + B \cdot t + C \cdot \mathrm{Sin}\left(\frac{2\pi}{12}t\right) + D \cdot \mathrm{Cos}\left(\frac{2\pi}{12}t\right). \quad (33)$$

For each regression method, the mean slope of the 500 simulated time series was computed and plotted versus the mean yearly amplitude. Results from the base simulation of five years (60 points) and zero slope are shown in Figs. 9–11. Since the simulated time series had no long-term linear trend, any deviation of the mean slope from zero indicates a bias. The AR and MSR regressions are much less biased than the WLS regression, with mean slope values 2–4 times smaller than WLS (Fig. 9). The AR regression has a slightly smaller bias than the MSR for the base simulation. The variability of the slope estimates is comparable (Fig. 10), with WLS having slightly smaller variability than AR or MSR. The standard deviations of the WLS and AR slope estimates (Fig. 10) are within the theoretical standard error estimates for the slope (Fig. 11). Note that the theoretical AR standard error for the slope from Fig. 11 is in excellent agreement with the measured slope variability from the

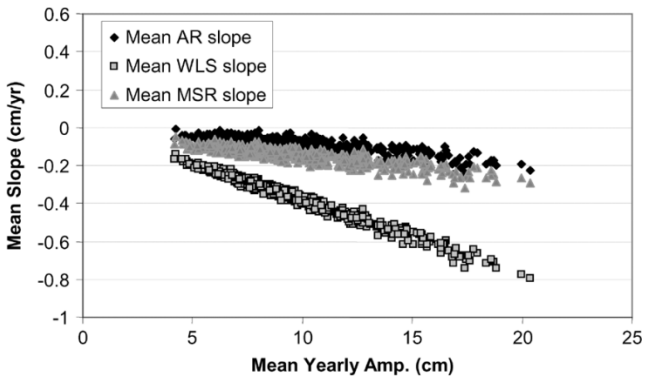

Fig. 9. Average slope of 500 Monte Carlo simulated zero-slope five-year elevation change time series versus average yearly amplitude of the five-year time series. Any deviation from zero slope indicates algorithm bias. The AR and MSR regressions are much less biased than the WLS regression, with mean slope values 2–4 times smaller than WLS. The AR regression has a slightly smaller bias than the MSR for the five-year base simulation.

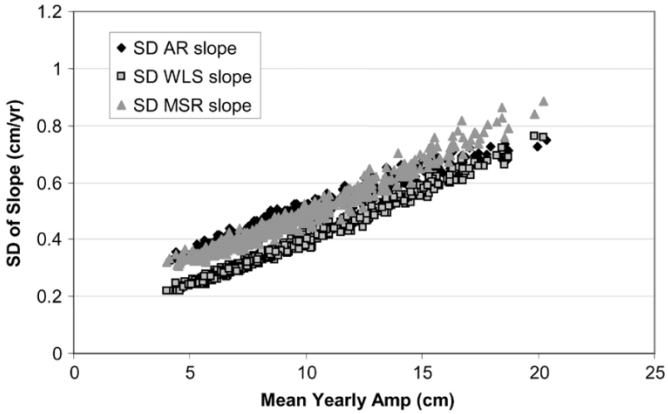

Fig. 10. Standard deviation of the slope from 500 Monte Carlo simulated zero-slope five-year elevation change time series versus average yearly amplitude of the five-year time series. The variability of the slope estimates is comparable, with WLS having slightly smaller variability than AR or MSR.

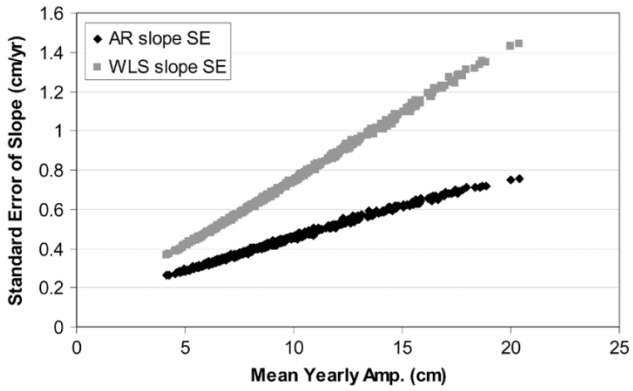

Fig. 11. Average theoretical SE estimates (Section III-C) for the Monte Carlo simulation results shown in Figs. 9 and 10. The standard deviations of the WLS and AR slope estimates (Fig. 10) are within the theoretical standard error estimates shown here. However, note that the theoretical AR slope standard error is in excellent agreement with the measured slope variability (Fig. 10), whereas the theoretical WLS slope standard error severely overestimates the actual slope variability (Fig. 10).

and AR slope estimates (Fig. 10) are within the theoretical standard error estimates for the slope (Fig. 11). Note that the theoretical AR standard error for the slope from Fig. 11 is in excellent agreement with the measured slope variability from the

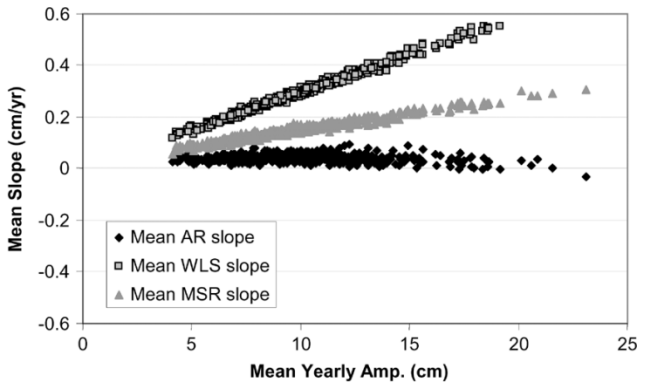

Fig. 12. Average slope of 500 Monte Carlo simulated zero-slope 5.5-year elevation change time series versus average yearly amplitude of the 5.5-year time series. Any deviation from zero slope indicates algorithm bias. The AR regression has essentially zero bias whereas the WLS and MSR regressions have significant biases, especially for large cycle amplitudes. Note that the MSR algorithm's bias is significantly larger than the results shown in Fig. 9 due to the addition of the extra half-cycle (5.5-year versus five-year) in this simulation.

Monte Carlo simulations in Fig. 10. This empirically validates the theoretical AR slope standard error derived in Section III-C. Conversely, note that the theoretical WLS standard error for the slope (Fig. 11) is nearly double that of the slope variability obtained from the Monte Carlo simulations (Fig. 10). This is because the white-noise assumption is invalid for WLS when applied to a strongly cyclical signal.

Additional Monte Carlo simulations were performed under a variety of conditions. We simulated 5.5-year time series to examine the effect of an additional half-cycle on the bias performance of the three algorithms. Here, the results in Fig. 12 indicate the AR method is clearly the least biased of the algorithms. Note that the MSR algorithm bias is substantially larger than the AR algorithm bias whereas there was only a small difference between the two in the five-year base simulation (Fig. 9). Thus, the additional half-cycle causes the MSR algorithm with constant yearly amplitude (33) to perform substantially worse. Results from a ten-year time series simulation are consistent with the five-year results except that the slope variability and bias are smaller because the interannual variations tend to average out over longer time series. The relative performance of the three algorithms with respect to the bias was consistent with the results shown in Fig. 9.

A final variation on the Monte Carlo simulations was to add gaps to the simulated five-year series. The quantity and location of gaps was selected to match the distribution of gaps found in five-year ERS-2 time series data from Antarctica [9]. The number of gaps was chosen from a Rayleigh distribution approximating the observed distribution, and the gap locations were picked from a uniform distribution that also approximated the observed distribution [18]. Results from this simulation did not differ significantly from the five-year base simulation results shown previously.

V. Conclusion

Analysis of ice sheet time series from satellite altimetry is complicated because typical elevation change time series will have: 1) a yearly cycle superimposed upon a longer term trend; 2) interannual variability of the cycle's amplitude; 3) missing points or gaps in the time series; and 4) variable standard errors for individual time series points (e.g., heteroscedasticity). Appropriate characterization of seasonal and interannual variations in the elevation change time series is essential for an accurate statistical evaluation of the longer term trends related to ice sheet mass balance, climate change, and global sea level rise.

In this paper, we presented an autoregressive model that could characterize both seasonal and interannual variations in ice sheet elevation change time series. The AR model was used in conjunction with weighted least squares regression to accurately estimate longer term linear trends present in the cyclically varying elevation change time series. This approach is robust in that it can account for seasonal and interannual elevation change variations, missing points in the time series, signal aperiodicity, time series heteroscedasticity, and time series with a noninteger (e.g., 5.5 year) number of yearly cycles. In addition, we derived a theoretically valid estimate of the uncertainty (standard error) in the long-term linear trend. Monte Carlo simulations were conducted that closely emulated actual characteristics of five-year elevation change time series from Antarctica [9], [18]. The Monte Carlo results indicated that the autoregressive approach yielded long-term linear trends that were less biased than two other approaches that have been recently used for analysis of ice sheet elevation change time series. In addition, the simulation results demonstrate that the variability (uncertainty) of the long-term linear trend estimates from the AR approach is in very good agreement with the theoretical standard error estimates derived in Section III-C.

NASA's ICESat laser altimeter began operation in 2003 (http://icesat.gsfc.nasa.gov), and ESA's CryoSat advanced radar altimeter is scheduled for launch in mid 2005 (http://www.esa.int/esaLP/cryosat.html). ICESat has extended coverage of the polar ice sheets up to latitudes of $\pm 86^\circ$ and CryoSat will further extend coverage to $\pm 88^\circ$ [19]. These instruments will provide important new observations of coastal areas and outlet glaciers where previous satellite radar altimeter measurements are sparse and of limited utility. Both ICESat and CryoSat were planned for nominal three-year mission lifetimes. However, ICESat's first of three lasers failed in March of 2003 after only one month of science data collection, and a revised mission plan was subsequently developed where the other two lasers will be turned on only periodically to collect science data. Thus, ICESat's current operational state combined with 30% to 50% loss of data due to cloud cover will likely result in sparsely populated short duration time series. Consequently, analysis of ICESat laser altimeter time series for estimation of longer term linear trends will be more complicated and involve greater uncertainty than longer duration radar altimeter time series. The AR approach presented here is a robust and useful tool for modeling and analysis of both laser and radar ice sheet elevation change time series. The ability of the AR approach to accurately quantify the uncertainty in longer term linear trend estimates will be particularly useful for analysis of short duration and sparsely populated ice sheet elevation change time series expected from the ICESat mission. The AR approach could also be useful for short duration elevation change time series expected from the CryoSat mission as well.

REFERENCES

[1] C. J. van der Veen and J. F. Bolzan, "Interannual variability in net accumulation on the Greenland ice sheet: Observations and implications for mass balance measurements," *J. Geophys. Res.*, vol. 104, no. D2, pp. 2009–2014, 1999.

[2] E. Rignot and R. H. Thomas, "Mass balance of the polar ice sheets," *Science*, vol. 297, pp. 1502–1506, 2002.

[3] D. J. Wingham, A. J. Ridout, R. Scharroo, R. J. Arthern, and C. K. Shum, "Antarctic elevation change from 1992 to 1996," *Science*, vol. 282, pp. 456–458, 1998.

[4] E. Rignot, "Fast recession of a west Antarctic glacier," *Science*, vol. 281, pp. 549–551, 1998.

[5] H. J. Zwally, W. Abdalati, T. Herring, K. Larson, J. Saba, and K. Steffen, "Surface melt-induced acceleration of Greenland ice sheet flow," *Science*, vol. 297, pp. 218–222, 2002.

[6] H. J. Zwally and A. C. Brenner, " Ice sheet dynamics and mass balance," in *Satellite Altimetry and Earth Sciences: A Handbook of Techniques and Applications*. Orlando, FL: Academic, 2001, ch. 9, pp. 351–369.

[7] C. H. Davis and D. M. Segura, "An algorithm for time-series analysis of ice sheet surface elevations from satellite altimetry," *IEEE Trans. Geosci. Remote Sensing*, vol. 39, pp. 202–206, Jan. 2001.

[8] B. Legresy, F. Remy, and P. Schaeffer, "Different ERS altimeter measurements between ascending and descending tracks caused by wind induced features over ice sheets," *Geophys. Res. Lett.*, vol. 26, no. 15, pp. 2231–2234, 1999.

[9] C. H. Davis and A. C. Ferguson, "Elevation change of the Antarctic ice sheet, 1995–2000, from ERS-2 satellite radar altimetry," *IEEE Trans. Geosci. Remote Sensing*, vol. 42, Nov. 2004.

[10] R. J. Arthern, D. J. Wingham, and A. L. Ridout, "Controls on ERS altimeter measurements over ice sheets: Footprint-scale topography, backscatter fluctuations, and the dependence of microwave penetration depth on satellite orientation," *J. Geophys. Res.*, vol. 106, no. D24, pp. 33 471–33 484.

[11] C. H. Davis, R. G. Belu, and G. Feng, "Elevation change measurement of the east Antarctic ice sheet, 1978–1988, from satellite radar altimetry," *IEEE Trans. Geosci. Remote Sensing*, vol. 39, pp. 635–644, Mar. 2001.

[12] B. Legresy and F. Remy, "Using the temporal variability of satellite radar altimetric observations to map surface properties of the Antarctic ice sheet," *J. Glaciol.*, vol. 44, no. 147, pp. 197–206, 1998.

[13] D. Cochrane and G. H. Orcutt, "Applications of least squares regression to relationships containing autocorrelated errors," *J. Amer. Stat. Assoc.*, vol. 44, pp. 32–61, 1949.

[14] R. H. Shumway and D. S. Stoffer, *Time Series Analysis and Applications*. New York: Springer-Verlag, 2000.

[15] C. Chatfield, *The Analysis of Time Series: An Introduction*, 4th ed. New York: Chapman and Hall, 1989.

[16] H. Akaike, "A new look at statistical model identification," *IEEE Trans. Automat. Contr.*, vol. AC-19, pp. 716–723, 1974.

[17] R. Christensen, *Plane Answers to Complex Questions: The Theory of Linear Models*. New York: Springer-Verlag, 1996.

[18] A. C. Ferguson, "Time series analysis of ERS-2 elevation data for estimation of Antarctic ice sheet mass balance," M.S. thesis, Univ. Missouri-Columbia, Columbia, Aug. 2002.

[19] M. R. Drinkwater, R. Francis, G. Ratier, and D. J. Wingham, "The European Space Agency's earth explorer mission CryoSat: Measuring variability in the cryosphere," *Ann. Glaciol.*, vol. 39, to be published.

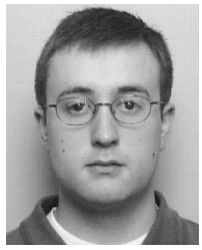

Adam C. Ferguson (S'00–M'02) was born in Sedalia, MO on September 25, 1979. He received the B.S. and M.S. degrees in electrical engineering from the University of Missouri-Columbia, in 2001 and 2002, respectively.

He is currently an RF Engineer in the Radar Engineering Department, National Nuclear Security Administration, Kansas City, MO (operated by Honeywell FM&T).

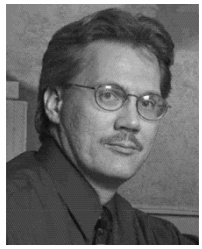

Curt H. Davis (S'90–M'92–SM'98) was born in Kansas City, MO, on October 16, 1964. He received the B.S. and Ph.D. degrees in electrical engineering from the University of Kansas, Lawrence, in 1988 and 1992, respectively.

He has been actively involved in experimental and theoretical aspects of microwave remote sensing of the ice sheets since 1987. He has participated in two field expeditions to the Antarctic continent and one to the Greenland ice sheet. From 1989 to 1992, he was a NASA Fellow at the Radar Systems and Remote Sensing Laboratory, University of Kansas where he conducted research on ice sheet satellite altimetry. He is currently the Croft Distinguished Professor of Electrical and Computer Engineering and Director of the Center for Geospatial Intelligence at the University of Missouri-Columbia. He is presently serving as a member of NASA's Interdisciplinary Science Team for global sea level assessment. His research interests are in the areas of mobile radio signal propagation, RF/microwave systems, satellite altimetry, remote sensing of the polar ice sheets, and remote sensing applications for urban environments.

Dr. Davis is a member of the Tau Beta Pi, Eta Kappa Nu, and URSI-Commission F. He is a former Chairman of the Instrumentation/Future Technologies committee of the IEEE Geoscience and Remote Sensing Society. In 1996, he was selected by the International Union of Radio Science for their Young Scientist Award. He was awarded the Antarctica Service Medal from the National Science Foundation. In 2002, he received the American Society of Photogrammetry and Remote Sensing President's Award for Practical Papers. He served as the Technical Program Co-Chairman of the 2004 IEEE Geoscience & Remote Sensing Symposium held in Anchorage, AK.

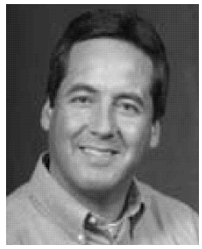

Joseph E. Cavanaugh was born in Spokane, WA on November 16, 1962. He received B.S. degrees in mathematics and computer science in 1986 from Montana Tech, the University of Montana, Butte, the M.S. degree in statistics in 1988 from Montana State University, Bozeman, and the Ph.D. in statistics in 1993 from the University of California, Davis.

He is currently an Associate Professor in the Department of Biostatistics, the University of Iowa, Iowa City. His research interests include model selection, time series analysis, linear models, modeling diagnostics, computational statistics, discrimination and classification, and missing data applications.